

Bell-inequality in path-entangled single photon and purity test

K. Muhammed Shafi,¹ R. S. Gayatri,¹ A. Padhye,¹ and C. M. Chandrashekar^{1,2,3,*}

¹*Quantum Optics & Quantum Information, Department of Instrumentation and Applied Physics, Indian Institute of Science, Bengaluru 560012, India*

²*The Institute of Mathematical Sciences, C. I. T. Campus, Taramani, Chennai 600113, India*

³*Homi Bhabha National Institute, Training School Complex, Anushakti Nagar, Mumbai 400094, India*

Different degrees of freedom of single photons have been entangled and used as a resource for various quantum technology applications. We present a scheme to perform Bell's test and show the violation of CHSH inequality in a path-entangled single photon state using non-interferometric approach in beam splitter setting. We demonstrate this experimentally by generating and controlling path-entangled state using single photons from spontaneous parametric down-conversion and performing non-interferometric measurements using two detector module. The transition from violation of CHSH inequality to validity is demonstrated when the purity of single photons state decrease below 70% visibility, $\mathcal{P} < 0.7$. Our procedure allows a purity test on any single photon source and to study quantum correlations on systems driven by dynamics where single particle entanglement with position space is prominent.

I. INTRODUCTION

Single photons and entangled photon pairs have been a very useful resource for several experimental tests of fundamentals of quantum physics [1, 2]. Lately, they have been extensively used for quantum technology applications [3–7]. Among different approaches, spontaneous parametric down-conversion (SPDC) is one of the matured methods to generate such photons [8]. Experimental feasibility to control various degrees of freedom of photons such as polarization [2, 9, 10], frequency [11], time-bin [12] and path [13–15] independently and simultaneously in different combinations have enabled generation of high-dimensional entangled states [16]. These higher dimensional entangled systems have shown significant improvement in processing quantum information. In contrast to the standard notion of entanglement that has been associated with two or more quantum systems [17–19], single-particle states are also known to exhibit quantum nonlocality [20–23]. This was further probed by a series of theoretical [24–32] and experimental investigations [33–39] establishing the single-particle entanglement to be between the spatial modes, rather than between the quantum systems. Over time, single-photon entangled states have also been widely used as a resource for quantum information processing [40–44] and quantum computation [45, 46].

For more than four decades since the proposal for Bell's test [17] and experimental violation of the Clauser, Horne, Shimony, and Holt (CHSH) inequality [47], innumerable experiments have been performed on various systems to establish quantum nonlocality, characterize entanglement between systems and between different degrees of freedom of a single particle. CHSH inequality violation with single photons entangled in momentum and polarization was shown using a Mach-Zehnder interfer-

ometer setting [48, 49]. Violation with photon entangled in polarization and orbital angular momentum [50] and using homodyne detection measurement scheme [51] has also been reported.

In this work we first present a theoretical scheme to show the violation of CHSH inequality in path-entangled single photon state using non-interferometric approach. The scheme involves the use of beam splitters to control the probability amplitude of presence and absence of photon along the two paths and to obtain the probabilities associated with the four basis states needed to calculate CHSH parameter. We also model decoherence in the form of depolarizing channel [52] and by introducing the presence of multi-photons in the source and show the transition from violation of CHSH inequality to its validity (thermal state) with decrease in purity of single photon state (visibility). We demonstrate this experimentally by employing a setup composing of a probabilistic single photon source from the SPDC using type-II Beta Barium Borate (BBO) crystal and two detector modules. Using combination of wave plates we have experimentally reduced the entanglement visibility and mimicked the reduction in purity of single photons (depolarizing channel) to show the transition from violation of CHSH inequality to validity with decrease in purity. Unlike the previous experimental reports of such results using interferometer setting for single photons [48, 49], our measurement procedure allows a sequence of measurements without the need for any interferometry approach which need more experimental resources. For any quantum communication and computation applications of single photons, purity of source is a key factor. A simple test for purity using CHSH inequality violation presented here will be a very useful resource and will also be useful to experimentally verify and study quantum correlations in systems where single particle dynamics are associated with spatial modes.

The paper is organized as follows. In Section II we present an analytical description of a path-entangled single photon in a beam splitter setup and the procedure

*Electronic address: chandracm@iisc.ac.in

to calculate CHSH parameter. After showing the violation of CHSH inequality we present a scheme to introduce tunability in splitting of photons along different paths using polarization degree of freedom as a control parameter. In Section III we present an experimental setup, the measurement procedure and the results showing the violation of CHSH inequality. We also present the transition from violation to satisfying inequality with decrease in purity of single photon state by using the tunable parameter in the experimental setup. In Section IV we conclude with our remarks.

II. THEORETICAL DESCRIPTION

A. Bell's-test for path-entangled single photon

Bell's test : Entangled photon pairs in polarization degree of freedom is given by,

$$|\Psi\rangle_{EP} = \frac{1}{\sqrt{2}} \left[|H\rangle_1 |V\rangle_2 + |V\rangle_1 |H\rangle_2 \right], \quad (1)$$

where $|H\rangle$ and $|V\rangle$ represent the polarization states and subscript represent the two photons. Standard Bell's test procedure on such entangled pairs involve rotation of polarization angle by θ and δ on each photon (two associated Hilbert spaces) independently just before they reach spatially separated detectors. Rotation of polarization angle results in spanning over all four basis states of the two photons. Then a series of coincidence events of detection in the form of $E(\theta, \delta)$ are recorded for different configurations of angles. Using those values, CHSH parameter

$$S = |E(\theta, \delta) - E(\theta, \delta')| + |E(\theta', \delta) + E(\theta', \delta')| \quad (2)$$

is calculated. If the value of $S > 2$, violation of CHSH inequality ($S \leq 2$) is observed suggesting nonlocal effect, an entangled state. Theoretically,

$$E(\theta, \delta) = P_{00} + P_{11} - P_{01} - P_{10} \quad (3)$$

where P_{ij} are the probabilities of different basis states of the composite system. Experimentally they can be obtained from coincidence counts of occurrence in different combination of basis states.

Path-entangled single photon : Path-entangled single photon state is generated when m spatial modes share a single photon. Then the state in m spatial mode will exist in a Hilbert space $\mathcal{H} = \bigotimes_{i=1}^m \mathcal{H}_i$, where \mathcal{H}_i is the Hilbert space of the i^{th} spatial mode. Each \mathcal{H}_i will be spanned by $\{|0\rangle_i, |1\rangle_i\}$ representing the photon occupancy, absence and presence of photon, respectively in the mode.

For a single photon passing through a 50:50 beam split-

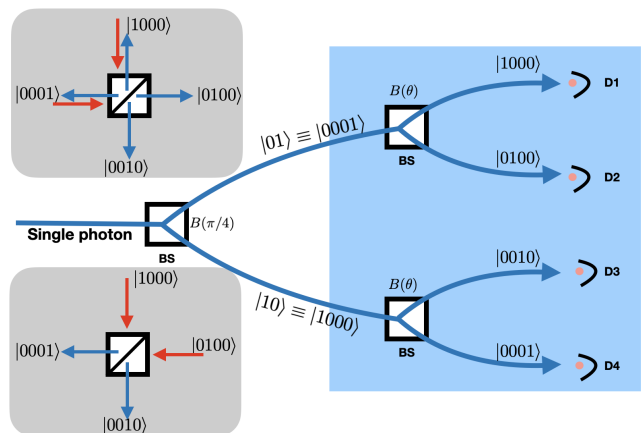


FIG. 1: Schematic representation of two input of the beam splitter to realize four and two output modes as basis states is presented in the inset. Its physical realization using combination of beam splitters is presented in the main schematic. The scheme comprises of beam splitters with different splitting ratio and four single photon counting module will allow us to control and span all four basis states and calculate CHSH parameter, Bell's test on a path-entangled single photon system.

ter, the path-entangled state will be in the form,

$$|\Psi\rangle_{1-2} = \frac{1}{\sqrt{2}} \left[|1\rangle_1 |0\rangle_2 + |0\rangle_1 |1\rangle_2 \right], \quad (4)$$

where the subscript 1 and 2 represent the two spatial modes or paths for the photon. To calculate CHSH parameter one has to span over all the basis states associated with the two spatial mode and photon occupancy. In two photon system described earlier using polarization state we can perform rotation on the polarization state of the photon and obtain non-zero probability of state $|HH\rangle$ and $|VV\rangle$. But in single photon occupancy description in two spatial mode, the states $|0\rangle_1 |0\rangle_2$ and $|1\rangle_1 |1\rangle_2$ will always have a zero probability amplitude. However, using single photon state along two different input modes all the four spatial modes of the beam splitter in occupancy representation with non-zero probability can be realized. The basis states in the Fock state representation can then be written as $|n_1, n_2, n_3, n_4\rangle$ and for a single photon case $n_1 + n_2 + n_3 + n_4 = 1$. This can be experimentally replicated by adding two identical beam splitters along the two output modes of the first beam splitter as show in Fig. 1. In the insets of Fig. 1 we also show the schematic of the beam splitters' spatial modes for single photon and combination of input states for realisation of four and two basis states, respectively. The generic output state in the photon occupancy representation will be,

$$|\Psi\rangle_{1-4} = a|1000\rangle + b|0100\rangle + c|0010\rangle + d|0001\rangle. \quad (5)$$

When any two output modes have non-zero probability, eliminating the redundant modes, the state will be identi-

cal to path-entangled single photon state given in Eq. (4).

Alternatively, the four basis states with non-zero probability from the two input spatial modes can also be re-written by associating each spatial modes, s_1 and s_2 with the *transmitted* and *reflected* component of the photon using states $|0\rangle_{s_i}$ and $|1\rangle_{s_i}$, respectively. In this representation all four basis states $\{|0\rangle_{s_1}|0\rangle_{s_2}, |0\rangle_{s_1}|1\rangle_{s_2}, |1\rangle_{s_1}|0\rangle_{s_2}, |1\rangle_{s_1}|1\rangle_{s_2}\}$ can be spanned by introducing single photon in superposition of two input modes of the beam splitter with variable θ controlling the splitting ratio. In two spatial mode representation, the state with all four basis states will be in the form,

$$|\Psi\rangle_{s_1-s_2} = a|0\rangle_{s_1}|0\rangle_{s_2} + b|0\rangle_{s_1}|1\rangle_{s_2} + c|1\rangle_{s_1}|0\rangle_{s_2} + d|1\rangle_{s_1}|1\rangle_{s_2}. \quad (6)$$

In Fig. 2 we show the combination of beam splitters to span over all four basis state in Hilbert space $s_1 \otimes s_2$ representation. First, the transmitted and reflected components from mode s_1 are spatially separated and it is further subjected to splitting using two beam splitters which represents spatial mode s_2 .

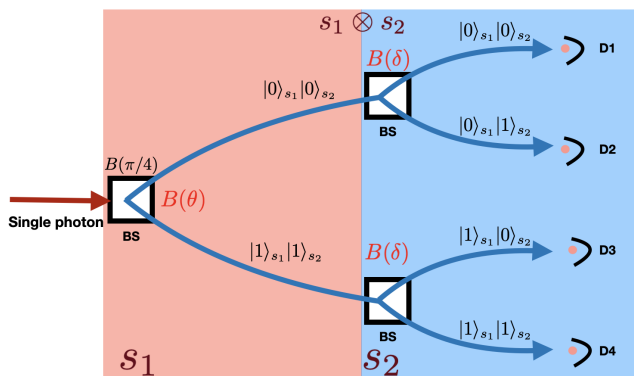


FIG. 2: Schematic representation of combination of beam splitter in two spatial mode representation which is identical to photon occupancy representation. Operators $B(\theta)$ and $B(\delta)$ on each mode will help in spanning over all four basis states and obtain probabilities to calculate CHSH parameter.

In Fig. 2, when second pair of beam splitter is absent, the state $|\Psi\rangle_{s_1-s_2}$ can be written as

$$|\Psi\rangle_{p-s} = \frac{1}{\sqrt{2}} \left[|0\rangle_{s_1}|0\rangle_{s_2} + |1\rangle_{s_1}|1\rangle_{s_2} \right]. \quad (7)$$

Since we only have access to change the splitting components along paths in both the description, we can only measure the probability of finding photon along each path. This results in an identical effect on both the representation showing the equivalence, $|\Psi\rangle_{1-4} \equiv |\Psi\rangle_{s_1-s_2}$. Therefore, for all practical purpose for path-entangled single photon in beam splitter setting,

$$|\Psi\rangle_{1-2} \equiv |\Psi\rangle_{p-s}. \quad (8)$$

Bell's test on path-entangled single photon : To perform Bell's test on photon in path-entangled state given by Eq. (4), we need to calculate $E(\theta, \delta)$. The parameter θ and δ will control the amplitudes of *presence* and *absence* of photon in two basis states associated with each of the paths and this can be realised using the beam splitter in operational form,

$$B(\theta) = \begin{bmatrix} \cos(\theta) & i \sin(\theta) \\ i \sin(\theta) & \cos(\theta) \end{bmatrix} \quad (9)$$

along each path. By measuring the probabilities along the four outputs paths of the beam splitter, $E(\theta, \delta)$ can be calculated. However, before calculating $E(\theta, \delta)$ we will first deliberate the equivalence of beam splitter operation on states in photon occupancy representation and in two spatial mode representation. In photon occupancy representation, any change in amplitude of *presence* (*absence*) of photon in one path directly affects the *absence* (*presence*) of the photon in the other path. Therefore, any change on path 1 using $B(\theta)$ will reflect on path 2 and any change on path 2 using $B(\delta)$ will reflect on path 1. In a generic description we can write down the state with controllable probability of presence of photon in each path in the form,

$$\begin{aligned} |\Psi\rangle_{1-4} &= \begin{bmatrix} B(\theta) & 0 \\ 0 & B(\theta) \end{bmatrix} \begin{bmatrix} B(\delta) & 0 \\ 0 & B(\delta) \end{bmatrix} \left[\frac{1}{\sqrt{2}} (|1000\rangle + |0001\rangle) \right] \\ &= \begin{bmatrix} B(\theta + \delta) & 0 \\ 0 & B(\theta + \delta) \end{bmatrix} \frac{1}{\sqrt{2}} \begin{bmatrix} 1 \\ 0 \\ 0 \\ 1 \end{bmatrix} \\ &= \frac{1}{\sqrt{2}} \begin{bmatrix} \cos(\theta + \delta) \\ i \sin(\theta + \delta) \\ i \sin(\theta + \delta) \\ \cos(\theta + \delta) \end{bmatrix}. \end{aligned} \quad (10)$$

In two spatial mode representation as described in Fig. 2 where states are represented using transmitted and reflected components along each path, the action of $B(\theta)$ and $B(\delta)$ will be in the form,

$$\begin{aligned} |\Psi\rangle_{s_1-s_2} &= \left(B(\theta) \otimes B(\delta) \right) |\Psi\rangle_{p-s} \\ &= \left(B(\theta + \delta) \otimes \mathbb{I} \right) |\Psi\rangle_{p-s} = \frac{1}{\sqrt{2}} \begin{bmatrix} \cos(\theta + \delta) \\ i \sin(\theta + \delta) \\ i \sin(\theta + \delta) \\ \cos(\theta + \delta) \end{bmatrix}. \end{aligned} \quad (11)$$

Since the probabilities associated with basis states in Eq. (10) and Eq. (11) are identical, equivalence between the two representation of single photon in the given beam splitter configuration can be established. Therefore, from the measurements outputs from the given setting, CHSH for path-entangled state can be calculated using spatial mode states. Here we would like to note that for a path-entangled photon along four output modes of single beam

splitter as show in the inset of Fig. 1, we will not have freedom to choose two different splitting ratio from the same beam splitter, we will have to consider $\theta = \delta$. However, in a generic setting using multiple beam splitters, we will have freedom to use both θ and δ .

The expression to calculate CHSH parameter in photon occupancy representation will be same as Eq. (2). In spatial mode setting due to the combined effect of beam splitter operation on spatial mode, $E(\theta, \delta) = E(\theta + \delta)$ and S will be,

$$S = |E(\theta + \delta) - E(\theta + \delta')| + |E(\theta' + \delta) + E(\theta' + \delta')|. \quad (12)$$

In Fig. 3 we show the CHSH parameter as function of θ

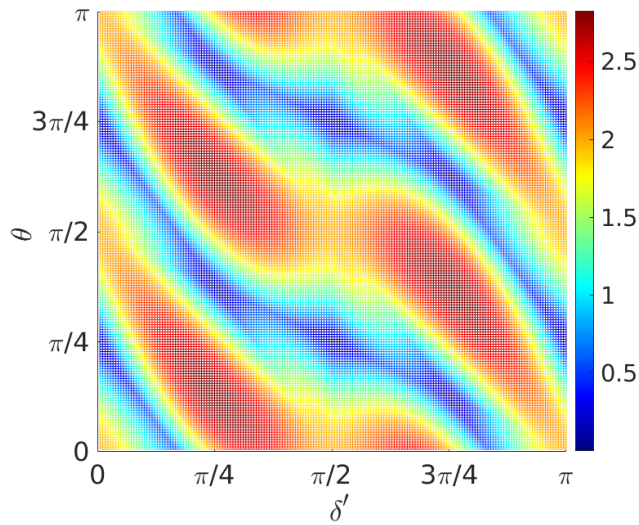


FIG. 3: CHSH parameter S as a function of θ and δ' in path-encoded single photon when $\delta = 0$ and $\theta' = (\theta + \delta')$. Violation of CHSH inequality ($S(\theta, \delta) > 2$) can be seen for range of combination of θ and δ' in a beam splitter scheme with four single photon detector module.

and δ' when $\delta = 0$ and $\theta' = (\theta + \delta')$. Using the probabilities, $E(\theta) = \cos(2\theta)$ and S parameter will be in the form,

$$S = |E(\theta) - E(\theta + \delta')| + |E(\theta + \delta') + E(\theta + 2\delta')|. \quad (13)$$

For several combination of parameters the value of $S(\theta, \delta) > 2$ is seen and the maximum value of $2\sqrt{2}$ is observed for four combination of (θ, δ') . For any initial state that is different from $|\Psi\rangle_{p-s}$ with different splitting ratio, one can use various combination of beam splitters along the two modes and show the violation of inequality. However, beam splitter setting gives limited access to perform Bell's test on states with varied splitting ratio between the paths. To perform Bell's test with more control over splitting ratio, we can use polarization degree of freedom where polarization rotator and polarization beam splitter (PBS) will give full control and serve as a

tool box to control photon splitting ratio along the paths.

The scheme for generation of a path-entangled single photon and perform Bell's test using polarization degree of freedom will be identical to Fig. 2. The splitting ratio is controlled using the polarization rotator (or half-wave plate (HWP)) and PBS. The basis states described earlier in this section, $\{|0\rangle_{s_1}, |1\rangle_{s_1}\}$ will be replaced with the basis states for polarization degree of freedom, $|H\rangle$ and $|V\rangle$. The rotation operation on polarization degree of freedom is given by

$$R(\theta) = \begin{bmatrix} \cos(\theta) & -\sin(\theta) \\ \sin(\theta) & \cos(\theta) \end{bmatrix}. \quad (14)$$

Rotating the state of photon $|H\rangle$ by angle $\theta = \pi/4$ we obtain $\frac{1}{\sqrt{2}}(|H\rangle + |V\rangle)$ and after passing it through PBS we will have a photon in path-entangled state in the form of $|\Psi\rangle_{p-s}$ as given in Eq. (7). To perform Bell's test we will choose two angle of rotations, θ to act on the Hilbert space associated with s_1 , photon polarization and δ on the Hilbert space associated with spatial mode s_2 . Since the action of operator on one spatial model will also be an action on the other spatial degree of freedom, the effective state will be,

$$\begin{aligned} |\Psi\rangle_{s_1-s_2} &= (R(\delta) \otimes \mathbb{I})(R(\theta) \otimes \mathbb{I})|\Psi\rangle_{p-s} \\ &= [R(\theta + \delta) \otimes \mathbb{I}]|\Psi\rangle_{p-s} = \frac{1}{\sqrt{2}} \begin{bmatrix} \cos(\theta + \delta) \\ \sin(\theta + \delta) \\ -\sin(\theta + \delta) \\ \cos(\theta + \delta) \end{bmatrix}. \end{aligned} \quad (15)$$

The expression $E(\theta, \delta)$ which is a composition of proba-

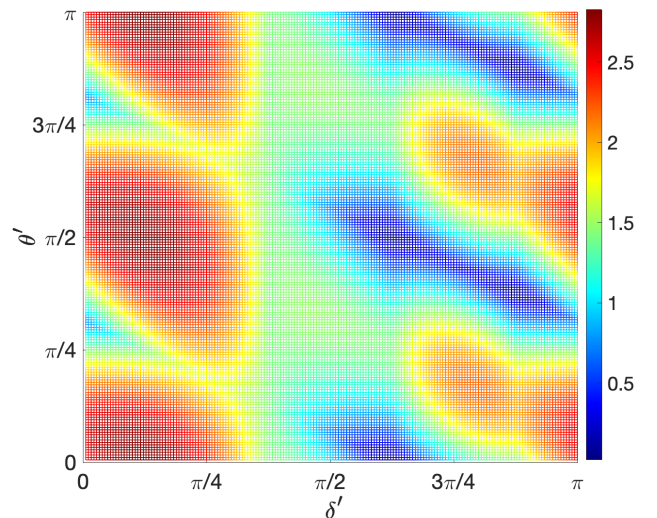


FIG. 4: CHSH parameter S as a function of θ' and δ' when θ and δ are fixed at $3\pi/4$ and $7\pi/8$. Violation of Bell's inequality ($S(\theta', \delta') > 2$) for various combination of θ' and δ' can be seen.

bility measurements in different basis state will be

$$E(\theta, \delta) = P_{00} + P_{11} - P_{01} - P_{10} = \cos 2(\theta + \delta). \quad (16)$$

CHSH parameter for different pairs of angles (θ, δ) and (θ', δ') will be,

$$S(\theta, \delta, \theta', \delta') = |E(\theta, \delta) - E(\theta, \delta')| + |E(\theta', \delta) + E(\theta', \delta')|. \quad (17)$$

In Fig. 4 the parameter $S(\theta', \delta')$ obtained when $\theta = 3\pi/4$ and $\delta = 7\pi/8$ is presented. Violation of CHSH inequality for various combination of parameters and a maximum violation of $S = 2\sqrt{2}$ is observed for some combination of parameters.

In addition to mimicking the path-entangled single photon, using the presence of polarization degree of freedom, a similar setup using the combination of beam splitter and PBS along with polarizer can be explicitly used to calculate CHSH parameter for polarization and path degree of freedom of single photon.

B. Purity test on single photon state

Depolarization : Transition of a pure quantum state to a maximally mixed state can be effectively modeled using quantum depolarizing channel. For the path-entangled single photon state, it is a linear combination of Eq. (7) in its density matrix form $\rho_{p-s} = |\Psi\rangle_{p-s}\langle\Psi|$ and maximally mixed state,

$$D_{\mathcal{P}}(\rho_{p-s}) = \mathcal{P}\rho_{p-s} + \frac{(1-\mathcal{P})}{2}\mathbb{I}. \quad (18)$$

Here $D_{\mathcal{P}}$ is a completely positive trace preserving map and \mathcal{P} is the probability or purity level in this case. By passing the state $\rho'_{p-s} = D_{\mathcal{P}}(\rho_{p-s})$ through additional pair of beam splitters, probabilities associated with all four basis states, $E(\theta, \delta)$ and CHSH parameter S can be calculated.

Multi-photon noise : One of the common cause for reduction in the purity of single photons is the probability of multi photon pair generation in some of the sources. When multi-photons accompany single photons, purity of single photons reduces and tends towards thermal state. When the photons source comprising of mixture of single photon and multi-photon states is passed through the beam splitter, the mixed input state can be written in the form,

$$\rho_m = \mathcal{P}(\rho_{p-s}) + \frac{(1-\mathcal{P})}{3}(\rho_1 + \rho_2 + \rho_3). \quad (19)$$

Here, ρ_{p-s} represents the single photons, $\rho_1 = (|01\rangle + |10\rangle)(\langle 01| + \langle 10|)$ represents multi photon detection in both the detectors, $\rho_2 = |01\rangle\langle 01|$ and $\rho_3 = |10\rangle\langle 10|$ rep-

resents unresolved multi-photon detection in either of the detector, respectively. The value of \mathcal{P} purity level of single photons in the mixed input state. The path-entangled state for the mixed input state is further passed through a pair of beams splitter to calculate CHSH parameter associated with the input state.

In Fig. 5 the maximum value for CHSH parameter obtained from numerical calculation with increase in purity of single photon state is shown. Increase in the value of S and violation of CHSH inequality can be recorded for $\mathcal{P} > 0.7$.

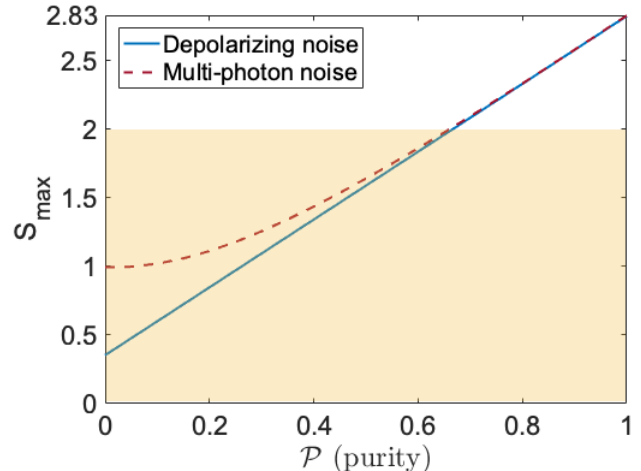


FIG. 5: Maximum value of S parameter with increase in purity (\mathcal{P}) of single photons when subjected to depolarizing noise and when the input state is a mixture of single and multi-photon states. For \mathcal{P} close to 0.7 we see the transition from validity of CHSH inequality to violation of CHSH inequality.

III. EXPERIMENTAL METHOD

In SPDC process photons are generated in pairs and presence of single photon can be gated by heralding the other photon. Since SPDC is probabilistic in nature, we will have time windows with single photons, no photons or multi-photons. Therefore, if we are not gating the presence of photon by heralding, the field striking the beam splitter is treated as a thermal source when one examines the full temporal behaviour. Instead of examining the full temporal behaviour, if we examine the field and photons detection in the smaller time windows we can resolve and record more single photons. Experimentally, with a choice of low pump power, small time window, better detector efficiency with low dead time and by filtering of the pump power from entering detector, one can resolve and detect more single photons even when it is not heralded. For our experiment we have chosen un-heralded source with a low pump power such that the minimum difference between the two detection obtained

by averaging over many trial runs is slightly higher than the detector dead time. Keeping the average minimum difference as a time window we resolve a good number of single photons. Though we will have many time window detecting no photons and a few window detecting multi-photons, single photon and no photon time windows outnumber giving us a random distribution of single photons over time.

A. Experimental setup

To experimentally demonstrate path-entangled single photon, a single photon generated from the SPDC process is used as a source. As per the schematic presented in Fig. 2 we will need four single photon detector modules (SPCM) for Bell's test. However, we will use only two detectors and measure the outcomes from only one of the basis of the path $|0\rangle_s$ as shown in Fig. 2. With a controlled initial state and series of measurements for different configurations we reproduce the full output expected from the four single photon counting module.

The schematic of an experimental setup is shown in Fig. 6. A 1-mm-long BBO nonlinear crystal cut for type-II phase-matching is pumped by a continuous-wave diode laser (Surelock, Coherent) at 405 nm with a pump power of 40 mW. A half-wave plate (HWP) is placed to control the pump polarization for optimal phase-matching. A plano-convex lens ($f=200$ mm) is used to tightly focus the laser into the crystal. Down-converted degenerate photons at 810 nm are collected using lens ($f=30$ mm) and passed through a bandpass interference filter (IF) at centre wavelength 810 nm with bandwidth of 10 nm FWHM to filter input pump. The generated orthogonal polarized photon pairs ($|H\rangle$, $|V\rangle$) are separated using a PBS and then coupled into single-mode fibers (SMF). Only horizontally ($|H\rangle$) polarized single photons with photon count of 4600 c/s at 40mW are used as our source to generate path-entangled photons.

A polarization controller, consisting of two quarter-wave plates (QWP) with a HWP in between, is used to maintain the initial polarization state of single photons to $|H\rangle$. In our setup, the polarization controller is also used as a depolarizing element to show the transition from validity of CHSH inequality to the violation of inequality with an increase in purity of quantum state of a single photon. To generate a path-entangled single photons and perform Bell's test measurements, splitting of photons along different paths are controlled using a combination of HWP and PBS. The single photon counting measurements in two paths are simultaneously performed using two SPCM ID120 from ID Quantique. By changing the HWP angle from 0 to 360 degrees, we recorded the photon counts in both paths. To test the purity of the photon state, we introduce depolarization channel by changing the angles in the waveplates present in polarization compensator. When the incident angle is not linearly polarized along the symmetry axis of the

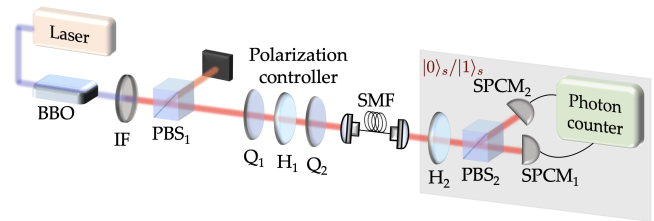


FIG. 6: Schematic of the experimental setup. A 405 nm laser pumps the BBO nonlinear crystal. The generated orthogonally polarized photon pairs ($|H\rangle$, $|V\rangle$) are separated using a polarization beam splitter (PBS₁). An interference filter (IF) at 810 nm center wavelength with a bandwidth of 10 nm FWHM is used for filtering the pump. A polarization controller, consisting of two quarter-wave plates (Q₁, Q₂) with a half-wave plate (H₁) in between, is used to maintain the initial polarization state of single photons to $|H\rangle$. The splitting of photons is controlled using a combination of a half-wave plate (H₂) and a polarization beam splitter (PBS₂). SPCM₁₋₂ are the two single photon counting module.

wave plate, the temporal walk-off will be acquired between the two polarization states. Though the detectors are insensitive to such short temporal walk-offs, the temporal distinguishability acquired during the propagation fulfils the role of the environment in general decoherence models [52]. Thus, by controlling the angles of the wave plates in polarization compensator, depolarization was introduced to change the visibility of photon state from 100% to 30%. Using the number of photon counts in each SPCM for all angles of HWP (H₂) we reconstruct the probability of finding photons in all four basis states of path-entangled single photon and calculate CHSH parameter.

B. Measurement procedure

In the experimental setup we have used combination of HWP and PBS to control the photon splitting along the paths and generate path-entangled state. The HWP operation can be written as

$$H(\kappa) = \begin{bmatrix} \cos(2\kappa) & \sin(2\kappa) \\ \sin(2\kappa) & -\cos(2\kappa) \end{bmatrix} \quad (20)$$

and when only probabilities of states are considered, $R(\theta) \equiv H(\kappa/2)$. To reproduce the probability output identical to the one obtained from Eq. (15), the HWP is set to rotate the state by $R(\theta + \delta)$ in different combinations and the combination that gives probabilities of all

four basis states are given below,

$$\begin{aligned}
 P_{00}(\theta, \delta) &= \frac{C_{D1}(\theta, \delta)}{C_{D1}(\theta, \delta) + C_{D1}(\theta_{\perp}, \delta_{\perp}) + C_{D2}(\theta, \delta) + C_{D2}(\theta_{\perp}, \delta_{\perp})} \\
 P_{10}(\theta, \delta) &= \frac{C_{D2}(\theta, \delta)}{C_{D1}(\theta, \delta) + C_{D1}(\theta_{\perp}, \delta_{\perp}) + C_{D2}(\theta, \delta) + C_{D2}(\theta_{\perp}, \delta_{\perp})} \\
 P_{11}(\theta, \delta) &= \frac{C_{D1}(\theta_{\perp}, \delta_{\perp})}{C_{D1}(\theta, \delta) + C_{D1}(\theta_{\perp}, \delta_{\perp}) + C_{D2}(\theta, \delta) + C_{D2}(\theta_{\perp}, \delta_{\perp})} \\
 P_{01}(\theta, \delta) &= \frac{C_{D2}(\theta_{\perp}, \delta_{\perp})}{C_{D1}(\theta, \delta) + C_{D1}(\theta_{\perp}, \delta_{\perp}) + C_{D2}(\theta, \delta) + C_{D2}(\theta_{\perp}, \delta_{\perp})}. \tag{21}
 \end{aligned}$$

$C_{D1}(\theta, \delta)$ and $C_{D2}(\theta, \delta)$ are the first set of number of photon counts in detector 1 and detector 2 when the rotation angles are θ and δ . $C_{D1}(\theta_{\perp}, \delta_{\perp})$ and $C_{D2}(\theta_{\perp}, \delta_{\perp})$ are the second set of number of photon counts in detector 1 and detector 2 when the rotation are θ_{\perp} and δ_{\perp} . From the probability values we calculate $E(\theta, \delta)$ and use that to obtain CHSH parameter S . Using the experimental data for number of photon counts detected per second averaged over 100 trials we calculate parameter $S(\theta', \delta')$ when θ and δ are fixed at $3\pi/4$ and $7\pi/8$.

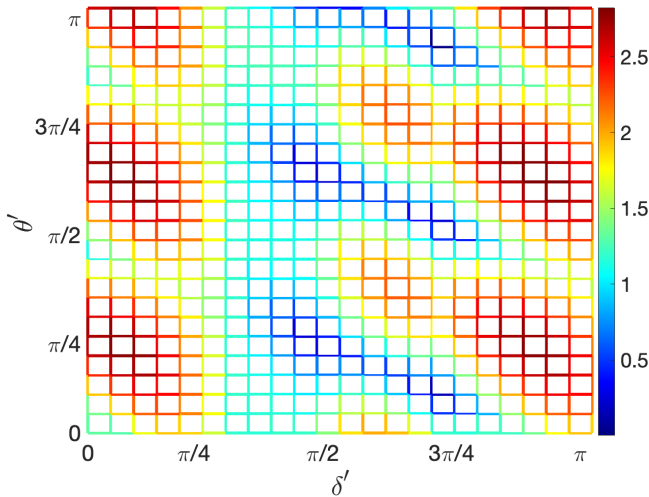


FIG. 7: CHSH parameter S as a function of θ' and δ' when θ and δ are fixed at $3\pi/4$ and $7\pi/8$. The plot is generated from the experimental photon counts obtained from two photon counting module. Violation of CHSH inequality ($S(\theta', \delta') > 2$) for various combination of values of θ' and δ' can be seen.

The output is shown in Fig. 7 and it is in agreement with the numerical simulation obtained for same parameters shown in Fig. 4. Using the data for full range of rotation of input state, we can reconstruct parameter S for any combination of θ , δ , θ' and δ' . The maximum value we could obtain from the experimental data is, $S = 2.82$. Due to simplicity of setup with minimum devices (optical components and detectors), the deviation from expected maximum value is very low. To calculate CHSH parameter for setup with different rotation, δ_1 and δ_2 along each path the first two probability values in Eq. (21) are calculated for δ_1 and second two probability values are calculated for δ_2 .

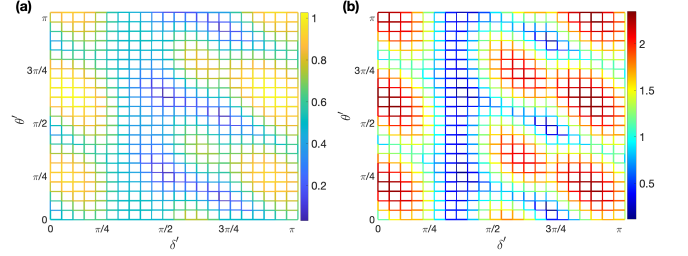


FIG. 8: CHSH parameter S as a function of θ' and δ' when θ and δ are fixed at $3\pi/4$ and $7\pi/8$. The plot is generated from the experimental photon counts (a) when visibility is 30% and (b) when visibility is 80%. Violation of inequality ($S(\theta', \delta') > 2$) for a range of values θ' and δ' can be seen when the visibility is 80% with maximum value of 2.35 and at 30% visibility, inequality is not violated.

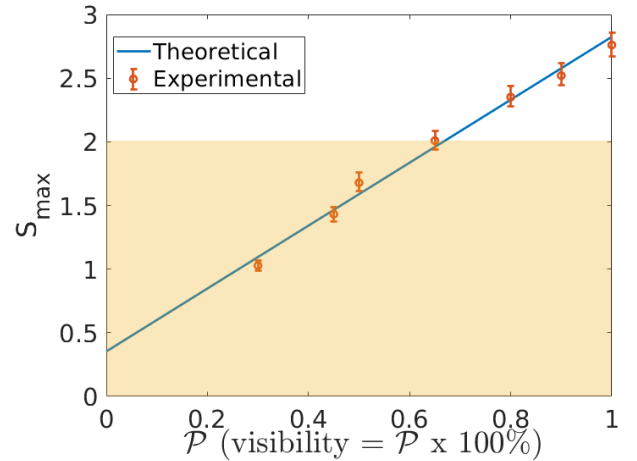


FIG. 9: Transition towards violation of CHSH inequality with increase in visibility. Theoretical expectation and experimental values for the maximum value of S when $\theta = 3\pi/4$ and $\delta = 7\pi/4$.

C. Test for purity of single photon state

Depolarizing channel with controllable parameters on single photon can be effectively realized using birefrin-

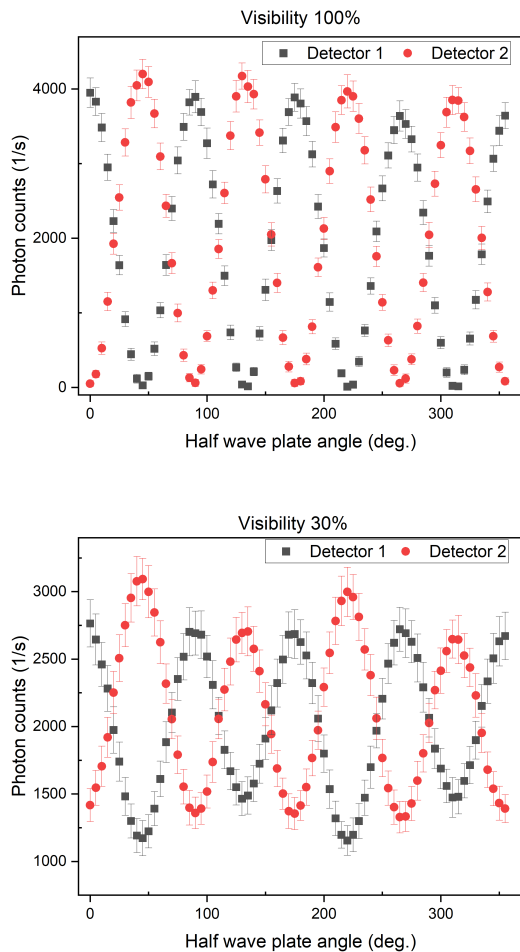


FIG. 10: Photon counts recorded in detector 1 and detector 2 with change in HWP angle when the visibility is 100% (pure state) and when the visibility is 30% (mixed state). Photons counts/ second was averaged over 100 trials.

gent crystals [52]. In path-entangled single photon state, transition from a pure state to a mixed quantum state can be seen with decrease in visibility of quantum state. Using the polarization compensator, QWP-HWP-QWP combination in the setup one can control the visibility (purity) of the quantum state by changing the angles in the polarization compensator. In Fig. 8 we show the value of CHSH parameter S from the experimental data for a set of values of θ and δ when visibilities are 30% and 80%, respectively. Though the pattern of change in S remains same for both visibility values, we can see a

significant difference in the value of S which is above 2 for 80% visibility and below 1 for 30% visibility. Fig. 9 illustrates the experimentally obtained value of S for different percentage of visibility along with the theoretical values of S as function of \mathcal{P} by introducing depolarizing channel as shown in Eq. (18). With an increase in purity \mathcal{P} , we clearly see the transition towards violation of CHSH inequality. In Fig. 10 we have provided the photon counts we recorded in two detectors with change in HWP angle when visibility of photon state was 100% and 30%.

IV. CONCLUSION

In this work we have presented a theoretical framework to calculate CHSH parameter for path-entangled single photons in beam splitter setting and has been experimentally demonstrated. By experimentally mimicking the effect of depolarizing channel, we have validated the use of CHSH as a test purity of single photon state. The theoretical results and experimental results we have obtained are in good agreement with each other. Though our theoretical scheme proposes the use of four detector (SPCM) module, we have used a measurement procedure that needs only two SPCM. The maximum value of CHSH parameter we have obtained is $S = 2.82$ and we have observed the transition towards violation of CHSH inequality happening around purity value of $\mathcal{P} = 0.7$ and above. In our procedure, polarization degree of freedom was only used to have control over the splitting of photon along different paths and was not explicitly used as one of degree of freedom to calculate CHSH parameter but same procedure will hold to calculate CHSH parameter for polarization and path degree of freedom. The simple non-interferometric scheme we have used for the demonstration makes it a practically efficient way to test purity of single photon state from any source. The measurement procedure we have adopted will be very useful to experimentally calculate quantum correlation in particle-path (spatial mode) entangled system. This work can lead to further investigations towards loophole free Bell's inequality [53] in path entangled or spatial mode setting, towards violation of CHSH inequality and still debated nonlocality effect in path-entangled state through quantum steering approach [54] and in temporal order [55].

Acknowledgment: We acknowledge the support from the Office of Principal Scientific Advisor to Government of India, project no. Prn.SA/QSim/2020.

-
- [1] R. H. Brown and R. Q. Twiss, Correlation between photons in two coherent beams of light, *Nature* **177**, 27-29 (1956).
 [2] P. G. Kwiat, K. Mattle, H. Weinfurter, A. Zeilinger, A. V. Sergienko, and Y. Shih, New High-Intensity Source of

- Polarization-Entangled Photon Pairs, *Phys. Rev. Lett.* **75**, 4337 (1995).
 [3] D. Bouwmeester, J.-W. Pan, K. Mattle, M. Eibl, H. Weinfurter, and A. Zeilinger, Experimental quantum teleportation, *Nature* **390**, 575-579 (1997.)

- [4] K. Mattle, H. Weinfurter, P. G. Kwiat, and A. Zeilinger, Dense Coding in Experimental Quantum Communication, *Phys. Rev. Lett.* **76**, 4656 (1996).
- [5] T. Jennewein, C. Simon, G. Weihs, H. Weinfurter, and A. Zeilinger, Quantum Cryptography with Entangled Photons, *Phys. Rev. Lett.* **84**, 4729 (2000).
- [6] J.-W. Pan, D. Bouwmeester, H. Weinfurter, and A. Zeilinger, Experimental Entanglement Swapping: Entangling Photons That Never Interacted, *Phys. Rev. Lett.* **80**, 3891 (1998).
- [7] X.-s. Ma, S. Zotter, J. Kofler, R. Ursin, T. Jennewein, C. Brukner, and A. Zeilinger, Experimental delayed-choice entanglement swapping, *Nature Phys* **8**, 479-484 (2012).
- [8] C. Couteau, Spontaneous parametric down-conversion, *Contemporary Physics* **59**(3), 291-304 (2018).
- [9] C. E. Kuklewicz, M. Fiorentino, G. Messin, F. N. C. Wong, and J. H. Shapiro, High-flux source of polarization-entangled photons from a periodically poled KTiOPO₄ parametric down-converter, *Phys. Rev. A* **69**, 013807 (2004).
- [10] M. Fiorentino, C. E. Kuklewicz and F. N. C. Wong, Source of polarization entanglement in a single periodically poled KTiOPO₄ crystal with overlapping emission cones, *Opt. Express* **13**, 127-135 (2005).
- [11] S. Ramelow, A. Fedrizzi, A. Poppe, N. K. Langford, and A. Zeilinger, Polarization-entanglement-conserving frequency conversion of photons, *Phys. Rev. A* **85**, 013845 (2012).
- [12] M. A. M. Versteegh, M. E. Reimer, A. A. van den Berg, G. Juska, V. Dimastrodonato, A. Gocalinska, E. Pelucchi, and V. Zwiller, Single pairs of time-bin-entangled photons, *Phys. Rev. A* **92**, 033802 (2015).
- [13] M. Krenn, A. Hochrainer, M. Lahiri, and A. Zeilinger, Entanglement by Path Identity, *Phys. Rev. Lett.* **118**, 080401 (2017).
- [14] J. Kysela, M. Erhard, A. Hochrainer, M. Krenn, and A. Zeilinger, Path identity as a source of high-dimensional entanglement, *Proceedings of the National Academy of Sciences of the United States of America* **117**(42), 26118-26122 (2020).
- [15] P. Caspar, E. Verbanis, E. Oudot, N. Maring, F. Samara, M. Caloz, M. Perrenoud, P. Sekatski, A. Martin, N. Sangouard, H. Zbinden, and R. T. Thew, Heralded Distribution of Single-Photon Path Entanglement, *Phys. Rev. Lett.* **125**, 110506 (2020).
- [16] M. Erhard, M. Krenn and A. Zeilinger, Advances in high-dimensional quantum entanglement, *Nat. Rev. Phys.* **2**, 365-381 (2020).
- [17] J. S. Bell, On the Einstein Podolsky Rosen paradox, *Physics Physique Fizika* **1**, 195 (1964).
- [18] J. F. Clauser and A. Shimony, Bell's theorem : experimental tests and implications, *Rep. Prog. Phys.* **41**, 1881 (1978).
- [19] A. Aspect, Bell's inequality test: more ideal than ever, *Nature* **398**, 189-190 (1999).
- [20] S. M. Tan, D. F. Walls, and M. J. Collett, Nonlocality of a single photon, *Phys. Rev. Lett.* **66**, 252 (1991).
- [21] L. Hardy, Nonlocality of a Single Photon Revisited, *Phys. Rev. Lett.* **73**, 2279 (1994).
- [22] D. M. Greenberger, M. A. Horne, and A. Zeilinger, Nonlocality of a Single Photon ?, *Phys. Rev. Lett.* **75**, 2064 (1995).
- [23] Lev Vaidman, Nonlocality of a Single Photon Revisited Again, *Phys. Rev. Lett.* **75**, 2063 (1995).
- [24] K. Banaszek and K. Wodkiewicz, Testing Quantum Nonlocality in Phase Space, *Phys. Rev. Lett.* **82**, 2009 (1999).
- [25] H. -W. Lee and J. Kim, Quantum teleportation and Bell's inequality using single-particle entanglement, *Phys. Rev. A* **63**, 012305 (2000).
- [26] G. Bjork, P. Jonsson, and L. L. Sánchez-Soto, Single-particle nonlocality and entanglement with the vacuum, *Phys. Rev. A* **64**, 042106 (2001).
- [27] S. J. van Enk, Single-particle entanglement, *Phys. Rev. A* **72**, 064306 (2005).
- [28] J. Dunningham and V. Vedral, Nonlocality of a Single Particle, *Phys. Rev. Lett.* **99**, 180404 (2007).
- [29] J. J. Cooper and J. A. Dunningham, Single particle nonlocality with completely independent reference states, *New J. Phys.* **10**, 113024 (2008).
- [30] J. B. Brask, R. Chaves, and N. Brunner, Testing nonlocality of a single photon without a shared reference frame, *Phys. Rev. A* **88**, 012111 (2013).
- [31] P. Abiuso, T. Kriváchy, E. Boghiu, M. Renou, A. Pozas-Kerstjens, A. Acín, Quantum networks reveal single-photon nonlocality, [arXiv:2108.01726 \[quant-ph\]](https://arxiv.org/abs/2108.01726).
- [32] A. Aiello, A Simple Field Theoretic Description of Single-Photon Nonlocality, [arXiv:2110.12930 \[quant-ph\]](https://arxiv.org/abs/2110.12930). 2110.12930.
- [33] E. Lombardi, F. Sciarrino, S. Popescu, and F. De Martini, Teleportation of a Vacuum-One-Photon Qubit, *Phys. Rev. Lett.* **88**, 070402 (2002).
- [34] F. Sciarrino, E. Lombardi, G. Milani, and F. De Martini, Delayed-choice entanglement swapping with vacuum-one-photon quantum states, *Phys. Rev. A* **66**, 024309 (2002).
- [35] S. A. Babichev, J. Ries and A. I. Lvovsky, Quantum scissors: Teleportation of single-mode optical states by means of a nonlocal single photon, *Euro. Phys. Lett.* **64**, 1 (2003).
- [36] S. A. Babichev, B. Brezger, and A. I. Lvovsky, Remote Preparation of a Single-Mode Photonic Qubit by Measuring Field Quadrature Noise, *Phys. Rev. Lett.* **92**, 047903 (2004).
- [37] S. A. Babichev, J. Appel, and A. I. Lvovsky, Homodyne Tomography Characterization and Nonlocality of a Dual-Mode Optical Qubit, *Phys. Rev. Lett.* **92**, 193601 (2004).
- [38] B. Hessmo, P. Usachev, H. Heydari, and G. Björk, Experimental Demonstration of Single Photon Nonlocality, *Phys. Rev. Lett.* **92**, 180401 (2004).
- [39] K. S. Choi, H. Deng, J. Laurat, and H. J. Kimble, Mapping photonic entanglement into and out of a quantum memory, *Nature* **452**, 67-71 (2008).
- [40] J. -W. Lee, E. K. Lee, Y. W. Chung, H. -W. Lee, and J. Kim, Quantum cryptography using single-particle entanglement, *Phys. Rev. A* **68**, 012324 (2003).
- [41] D. Salart, O. Landry, N. Sangouard, N. Gisin, H. Herrmann, B. Sanguinetti, C. Simon, W. Sohler, R. T. Thew, A. Thomas, and H. Zbinden, Purification of Single-Photon Entanglement, *Phys. Rev. Lett.* **104**, 180504 (2010).
- [42] C. Simon and J.-W. Pan, Polarization Entanglement Purification using Spatial Entanglement, *Phys. Rev. Lett.* **89**, 257901 (2002).
- [43] N. Sangouard, C. Simon, H. de Riedmatten, and N. Gisin, Quantum repeaters based on atomic ensembles and linear optics, *Rev. Mod. Phys.* **83**, 33 (2011).
- [44] C. Perumangatt, A. Lohrmann, and A. Ling, Experimental conversion of position correlation into polarization en-

- tanglement, *Phys. Rev. A* **102**, 012404 (2020).
- [45] E. Knill, R. Laflamme and G. J. Milburn, A scheme for efficient quantum computation with linear optics, *Nature* **409**, 46-52 (2001).
- [46] S. Singh, P. Chawla, A. Sarkar and C. M. Chandrashekar, Universal quantum computing using single-particle discrete-time quantum walk, *Sci. Rep.* **11**, 11551 (2021).
- [47] J. F. Clauser, M. A. Horne, A. Shimony, and R. A. Holt, Proposed Experiment to Test Local Hidden-Variable Theories, *Phys. Rev. Lett.* **23**, 880 (1969).
- [48] B. R. Gadway, E. J. Galvez and F. De Zela, Bell-inequality violations with single photons entangled in momentum and polarization, *J. Phys. B: At. Mol. Opt. Phys.* **42**, 015503 (2008).
- [49] M. Pasini, N. Leone, S. Mazzucchi, V. Moretti, D. Pastorello, and L. Pavesi, Bell-inequality violation by entangled single-photon states generated from a laser, an LED, or a halogen lamp, *Phys. Rev. A* **102**, 063708 (2020).
- [50] A. Vallés, V. D'Ambrosio, M. Hendrych, M. Micuda, L. Marrucci, F. Sciarrino, and J. P. Torres, Generation of tunable entanglement and violation of a Bell-like inequality between different degrees of freedom of a single photon, *Phys. Rev. A* **90**, 052326 (2014).
- [51] S. -Y. Lee, J. Park, J. Kim, and C. Noh, Single-photon quantum nonlocality: Violation of the Clauser-Horne-Shimony-Holt inequality using feasible measurement setups, *Phys. Rev. A* **95**, 012134 (2017).
- [52] A. Shaham and H. S. Eisenberg, Realizing controllable depolarization in photonic quantum-information channels, *Phys. Rev. A* **83**, 022303 (2011).
- [53] B. Hensen, H. Bernien, A. E. Dréau, A. Reiserer, N. Kalb, M. S. Blok, J. Ruitenberg, R. F. L. Vermeulen, R. N. Schouten, C. Abellán, W. Amaya, V. Pruneri, M. W. Mitchell, M. Markham, D. J. Twitchen, D. Elkouss, S. Wehner, T. H. Taminau and R. Hanson, Loophole-free Bell inequality violation using electron spins separated by 1.3 kilometres, *Nature* **526**, 682-686 (2015).
- [54] M. Ruzbehan, Simulation of the Bell inequality violation based on quantum steering concept, *Sci. Rep.* **11**, 5647 (2021).
- [55] M. Zych, F. Costa, I. Pikovski and C. Brukner, Bell's theorem for temporal order, *Nat. Commun.* **10**, 3772 (2019).